IL NUOVO CIMENTO Vol. 34 C, N. 4 Luglio-Agosto 2011
DOI 10.1393/ncc/i2011-10910-2

Colloquia: Channeling 2010

# Improvement in the performance of the X-ray source based on parametric X-ray radiation using a wedge-shaped target crystal

Y. Hayakawa(1)(2)(*), K. Hayakawa(1)(2), M. Inagaki(1)(2), T. Kuwada(1)(3), K. Nakao(1)(2), K. Nogami(1)(2), I. Sato(1)(4), Y. Takahashi(1)(3) and T. Tanaka(1)(2)

(1) *Laboratory for Electron Beam Research and Application, Nihon University 7-24-1 Narashinodai, Funabashi, 274-8501 Japan*

(2) *Institute of Quantum Science, Nihon University - 7-24-1 Narashinodai, Funabashi 274-8501 Japan*

(3) *Research Institute of Sciences and Technology, Nihon University - 7-24-1 Narashinodai Funabashi, 274-8501 Japan*

(4) *Advanced Research Institute for the Sciences and Humanities, Nihon University 12-5 Gobancho, Chiyoda-ku, Tokyo, 102-8251 Japan*

(ricevuto il 22 Dicembre 2010; pubblicato online il 7 Luglio 2011)

**Summary.** — The properties of parametric X-ray radiation (PXR) emitted from a wedge-shaped Si(111) crystal plate were experimentally investigated using the PXR generator at the Laboratory for Electron Beam Research and Application (LEBRA) of Nihon University. The wedge surface was imposed on a symmetric-cut Si(111) plate and has an asymmetric cut-surface with respect to the (111) crystal planes. As a result of the experiment, it was found that the PXR intensity improved can be obtained suppressing the degradation of the X-ray performance using a wedge-shaped target. With this improvement, phase-contrast images without absorption contrast could be obtained from DEI images taken with the exposure of several-ten seconds. The reduction of the exposure time made it possible to carry out a computed tomography (CT) experiment by DEI within a practical machine time, and phase-contrast tomograms of a biological sample were obtained at the PXR energy of 17.5 keV.

PACS 41.60.-m – Radiation by moving charges.
PACS 41.50.+h – X-ray beams and x-ray optics.
PACS 87.59.-e – X-ray imaging.

(*) E-mail: yahayak@lebra.nihon-u.ac.jp

 

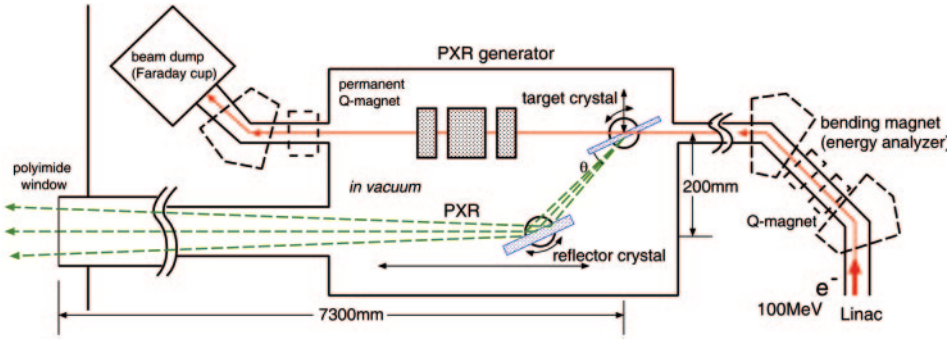


Fig. 1. – Schematic top view of the LEBRA-PXR generator equipped with a double-crystal system for tunability and its dedicated beamline.

## 1. – Introduction

A novel X-ray source based on parametric X-ray radiation (PXR) has been conducted at the Laboratory for Electron Beam Research and Application (LEBRA), Nihon University. The PXR source, which is equipped with a double-crystal system for tunability as shown in fig. 1, has been installed in a dedicated beamline connecting to a 125 MeV electron linac, and its tunable monochromatic X-ray beam has actually provided to user applications [1-3]. So far, the PXR beam in an energy range from 5 to 34 keV has been produced, using Si(111) or Si(220) planes as the radiation source [4, 5]. Since the PXR beam obtained from the LEBRA-PXR source has a large irradiation field, 100 mm in diameter, X-ray imaging at various X-ray energies have been the most popular application performed [6]. In particular, results of diffraction-enhanced imaging (DEI), which is a sort of X-ray phase-contrast imaging, have demonstrated the high performance of PXR with respect to spatial coherence [7, 8].

Due to the low repetition rate of the LEBRA linac, however, the average current of the electron beam is less than 5 $\mu$A. Thus, the properties of PXR emitted from asymmetrically cut target crystals have recently been studied to improve the intensity of the X-rays [9-11]. As the result of the increase of the available PXR intensity from the double-crystal system, the exposure required for adequate-quality imaging using ordinary image sensors such as an imaging plate has been reduced to several ten seconds [12]. The current specifications of the LEBRA-PXR source are listed in table I [13].

## 2. – Multi-beam effect at the edge of the target

Ordinary silicon perfect-crystal wafers with symmetric cut-surfaces have been used as the target crystal for PXR production since the advent of the LEBRA PXR source. Recently, target crystals with asymmetric cut-surfaces have been tested to increase the available X-ray yield. Figure 2(a) shows drawings of the symmetric and asymmetric target crystals. However, serious problems due to the geometrical effect of the target crystal have been found in both cases. When the edge of the target was irradiated with an electron beam, a strong image blur was observed in the imaging with a long propagation as shown in fig. 2(b) [14]. This phenomenon seems to result from the contributions of two X-ray beams at slightly different directions. Naturally, this effect seriously affects experiments requiring high accuracy such as DEI.

TABLE I. – *Typical parameters of the linac and the PXR generator of LEBRA.*

| | |
|---|---|
| Typical electron energy | 100 MeV |
| Accelerating frequency | 2856 MHz (*S*-band) |
| Macropulse beam current | 120–135 mA |
| Macropulse duration | 4–10 $\mu$s |
| Macropulse repetition rate | 2–5 pps |
| Bunch length | $\sim$ 3 ps |
| Average beam current at the linac exit | 1–5 $\mu$A |
| Range of the Bragg angle | 5.0–30° |
| PXR energy range | Si(111) target: 4.0–21 keV |
| | Si(220) target: 6.5–34 keV |
| Irradiation field size at the X-ray exit | 100 mm in diameter |
| Total X-ray photon rate | $10^6$–$10^8$ /s |

## 3. – Wedge-shaped crystal targets for PXR generation

Although the experimental results have suggested that the use of an asymmetric cut-surface has an advantage in terms of increasing the PXR intensity, the deterioration due to the multi-beam effect, which seems to depend on the side and reverse surfaces at the target edge, reduces the performance of the X-ray beam. Thus, new wedge-shaped crystal plates as shown in fig. 3(a) have been prepared to solve the problem and have been experimentally tested as PXR targets. An asymmetric cut-surface was made as a wedge-shaped surface on a symmetrically cut Si(111) plate. One of the wedge-shaped targets has a 1.15° wedge angle and the other has a 6.5° angle. Therefore, these targets have asymmetric cut-surfaces on the front side with asymmetric angles of 1.15° and 6.5°, respectively. In particular, the incident electrons graze the target at the PXR energy of 17.5 keV using the 6.5° wedge-shaped crystal.

In the imaging experiments using the same setup as in fig. 2(b), the image blur was suppressed using the new wedge-shaped targets. Figure 3(b) shows a typical result of the imaging experiments. Shaping the target edge as a wedge is a practical method for improving the PXR imaging quality.

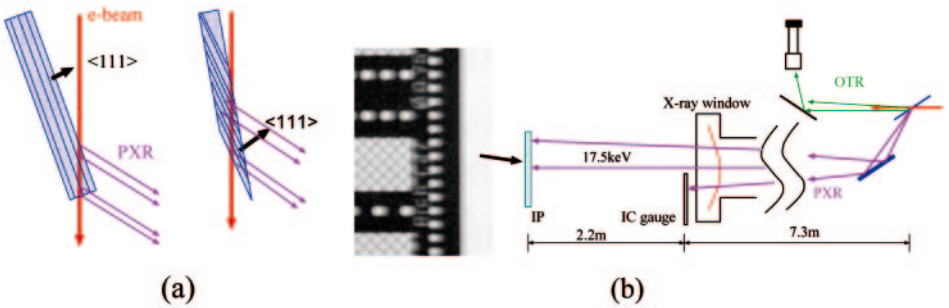


Fig. 2. – (a) Si target crystals with symmetric and asymmetric cut-surfaces with respect to the (111) plane. (b) Image blur observed in the imaging experiment with 2.2 m propagation between the sample (IC gauge) and the detector (imaging plate).

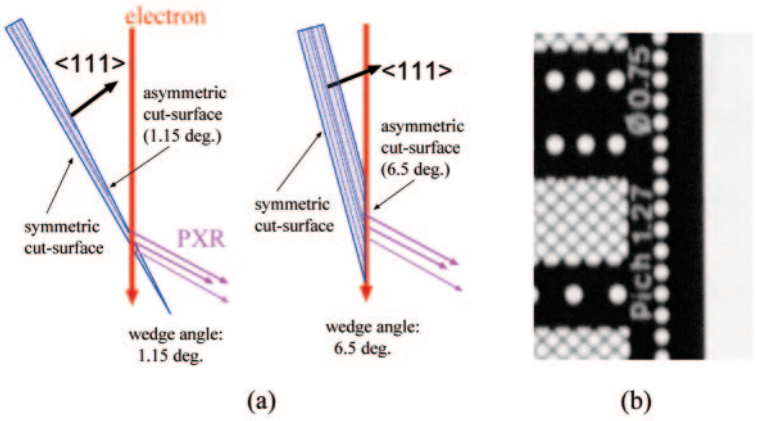


Fig. 3. – (a) Sketch of new wedge-shaped crystal plates for PXR targets with wedge angles of 1.15° and 6.5°. (b) A typical image observed in the same setup as in fig. 2(b) but using a wedge-shaped crystal target.

In addition to the imaging performance, the available X-ray yield was investigated using the wedge-shaped targets. The reverse case of the 6.5° wedge-shaped target, in which the symmetric cut-surface faces the incident electrons, was also tested as the reference. The relative PXR intensity from the double-crystal system using each target was measured using an ionizing-mode solid-state detector depending on the angle of the 2nd reflector crystal. These rocking curves at the PXR energy of 17.5 keV are shown in fig. 4(a). When the asymmetric cut-surface of the wedge-shaped edge faced the incident electrons, the widths of the rocking curves became narrower than that of the reverse case. In the front cases, therefore, the curves have higher peaks especially when the wedge angle is 6.5°. Since the LEBRA-PXR source is based on the double-crystal system, the peak height of the 2nd crystal's rocking curve represents the maximum X-ray yield that

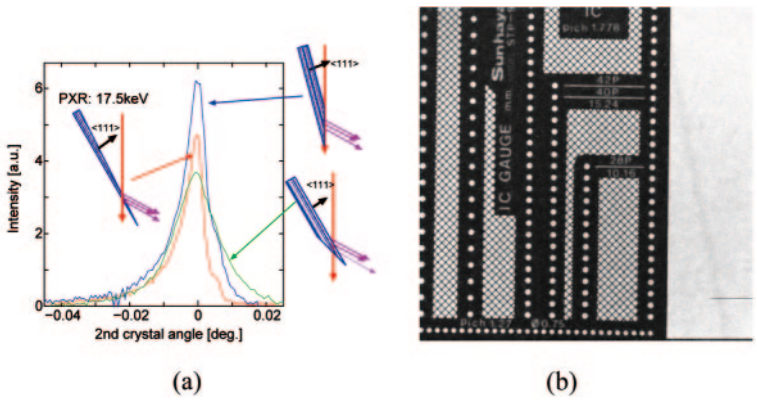


Fig. 4. – (a) The intensities of PXR from the double-crystal PXR generator using the new wedge-shaped targets measured as functions of the 2nd crystal's angle. (b) A typical PXR image obtained at the peak intensity of 17.5 keV using a flat-panel detector with 10 s exposure, where the average current of the electron beam at the target was 2.6 $\mu$A.

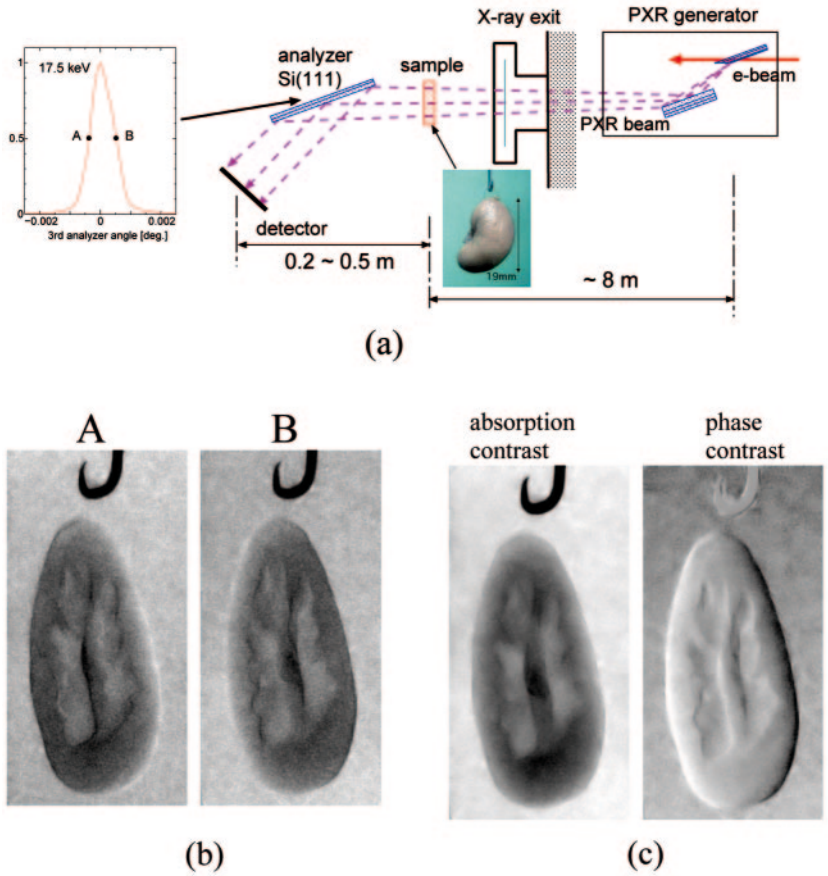


Fig. 5. – (a) The setup of the DEI experiment using the LEBRA-PXR source, where the phase-shift of X-rays due to the sample can be detected as the refraction angle of the X-rays using an analyzer of perfect crystal. (b) The typical DEI images of a mouse kidney obtained at the analyzer angles marked A and B on the rocking curve. (c) The absorption-contrast (left) and the phase-contrast (right) images obtained as the sum and difference of the two DEI images.

can be used for applications. Using the maximum yield at the energy of 17.5 keV with the 6.5° wedge-shaped target, ordinary X-ray images could be obtained with relatively short exposure times. The typical absorption image obtained using a flat-panel detector, which has a pixel size of 50 $\mu$m × 50 $\mu$m, with 10 s exposure is shown in fig. 4(b). If we can increase the electron beam current several times and/or use a detector with higher efficiency and lower noise, semi-real-time imaging with a frame rate of 1 /s may be possible in this condition.

## 4. – Computed tomography based on the DEI method

Since the image blur is suppressed and the available X-ray yield from the double-crystal system increases using the wedge-shaped target, the exposure required by obtaining the phase-contrast image by the DEI method is also reduced to several ten seconds. Figure 5(a) explains the DEI experiment using the LEBRA-PXR source, and the typical

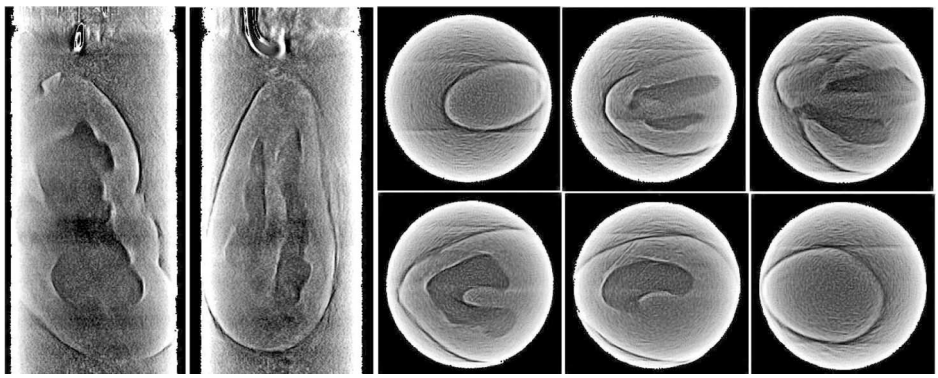

Fig. 6. – The tomograms reconstructed from 90 DEI projections obtained as shown in fig. 5. The total exposure was estimated to be 90 min.

DEI images of a biological sample are shown in fig. 5(b). Since DEI images provide the information about the X-ray refraction according to the analyzer angle, one can separate the absorption-contrast and the phase-contrast by calculating 2 DEI images [15, 16]. Figure 5(c) shows the sum and the difference of these DEI images, corresponding to the absorption-contrast and the phase-contrast images, respectively. Here, the exposure time of DEI images using an X-ray CCD camera was 30 s, and the total measurement time to obtain one phase-contrast image was 60 s. Since the image blur due to the multi-beam effect seriously disturbs the separation of phase-contrast from absorption-contrast, the use of a wedge-shaped target significantly improved the efficiency of such experiments.

In principle, computed tomography (CT) experiments based on the DEI method can be performed by rotating the sample. The reduced exposure required to obtain phase-contrast images makes such experiments practically possible within a machine time of the LEBRA linac. Actually, the DEI-CT experiment was carried out by a 2° angular step for the sample rotation, and the resulting tomograms reconstructed from 90 DEI projections are shown in fig. 6. Each projection was obtained in the same condition as fig. 5, and the total net measurement time was estimated to be 90 min. Although the artifact noise still remains in the tomogram, the differential images were actually obtained excluding the X-ray absorption. Unfortunately, the measurement system for the CT experiments has not yet been automatized, and the efficiency of the experiment is restricted by the manual work of data taking. It is expected that higher-quality tomograms for the same machine time could be obtained if an automatic measurement system were developed for the DEI-CT experiment.

## 5. – Conclusion

Using crystal plates with a wedged-shaped edge as the PXR target, the PXR intensity was improved suppressing the image blur due to the multi-beam effect of PXR emitted from the target edge. Due to this improvement, phase-contrast images without absorption contrast could be obtained from DEI images taken with an exposure of several ten seconds. The reduction of the exposure time made it possible to carry out CT experiments by DEI within a practical machine time, and phase-contrast tomograms of

a biological sample were achieved at the PXR energy of 17.5 keV. To our knowledge, this is the first case of successful phase-contrast CT using PXR.

* * *

This study on radiators of PXR was supported by by MEXT.KAKENHI (21686088). Studies on the imaging technique were also supported in part by MEXT.KAKENHI (21560055) and Nihon University Multidisciplinary Research Grant for 2009 (Sogo 09-024).

REFERENCES

[1] Hayakawa Y., Sato I., Hayakawa K. and Tanaka T., *Nucl. Instrum. Methods B*, **227** (2005) 32.
[2] Sakae T., Hayakawa Y., Mori A., Kuwada T., Sakai T., Nogami K., Tanaka T., Hayakawa K. and Sato I., *J. Miner. Petrol. Sci.*, **101** (2006) 10.
[3] Inagaki M., Hayakawa Y., Nogami K., Tanaka T., Hayakawa K., Sakai T., Nakao K. and Sato I., *Jpn. J. Appl. Phys.*, **47** (2008) 8081.
[4] Hayakawa Y., Sato I., Hayakawa K., Tanaka T., Mori A., Kuwada T., Sakai T., Nogami K., Nakao K. and Sakae T., *Nucl. Instrum. Methods B*, **252** (2006) 102.
[5] Hayakawa Y., Hayakawa K., Inagaki M., Kuwada T., Mori A., Nakao K., Nogami K., Sakae T., Sakai T., Sato I., Takahashi Y. and Tanaka T., in *Proceedings of SPIE Vol. 6634: International Conference on Charged and Neutral Particles Channeling Phenomena II (Rome)*, edited by Dabagov S. B. (SPIE, Washington) 2007, p. 663411.
[6] Sakae T., Takahashi Y., Hayakawa Y., Tanaka T., Hayakawa K., Kuwada T., Nakao K., Nogami K., Inagaki M., Sato I., Fukumoto M., Makimura M. and Yamamoto H., *J. Hard Tissue Biol.*, **19** (2010) 131.
[7] Fitzgerald R., *Phys. Today*, **53** (2000) 23.
[8] Takahashi Y., Hayakawa Y., Kuwada T., Sakai T., Nakao K., Nogami K., Inagaki M., Tanaka T., Hayakawa K. and Sato I., in *AIP Conference Proceedings 1221 "X-Ray Optics and Microanalysis"*, edited by Denecke M. and Walker C. T. (AIP, New York) 2010, p. 119.
[9] Feranchuk I. D. and Feranchuk S. I., *Eur. Phys. J. Appl. Phys.*, **38** (2007) 135.
[10] Blazhevich S. V. and Noskov A. V., *Nucl. Instrum. Methods B*, **266** (2008) 3777.
[11] Lobko A. S., Nasonov N., Park H., Piestrup M. and Zhukova P., in *Proceedings of SPIE Vol. 6634: International Conference on Charged and Neutral Particles Channeling Phenomena II (Rome)*, edited by Dabagov S. B. (SPIE, Washington) 2007, p. 663417.
[12] Hayakawa Y., Hayakawa K., Inagaki M., Kuwada T., Nakao K., Nogami K., Sakai T., Sato I., Takahashi Y. and Tanaka T., in *Proceedings of the 51st Workshop of the INFN Eloisatron Project "Charged and Neutral Particles Channeling Phenomena" Channeling 2008*, edited by Dabagov S. B. and Palumbo L. (World Scientific, Singapore) 2010, p. 677.
[13] Tanaka T., Hayakawa K., Hayakawa Y., Kuwada T., Sakai T., Nakao N., Takahashi Y., Nogami K., Inagaki M. and Sato I., in *AIP Conference Proceedings 1234 "SRI09 (The 10th International Conference of Synchrotron Radiation Instrumentation)"*, edited by Garrett R., Gentle I., Nugent K. and Wilkins S. (AIP, New York) 2010, p. 587.
[14] Hayakawa Y., Hayakawa K., Inagaki M., Kuwada T., Nakao K., Nogami K., Sakae T., Sakai T., Sato I., Takahashi Y. and Tanaka T., *Nucl. Instrum. Methods B*, **266** (2008) 3758.
[15] Davis T. J., Gao D., Gureyev T. E., Stevenson A. W. and Wilkins S. W., *Nature*, **373** (1995) 595.
[16] Ando M., Sugiyama H., Maksimenko A., Pattanasiriwisawa W., Hyodo K. and Zhan X., *Jpn. J. Appl. Phys.*, **40** (2001) L844.